SURFACE MICROSCOPY WITH LASERLESS MEMS BASED AFM PROBES

E. Algré, B. Legrand, M. Faucher, B. Walter, L. Buchaillot
IEMN, Institut d'Electronique, de Microélectronique et de Nanotechnologie,
CNRS UMR 8520 – Villeneuve d'Ascq, France

ABSTRACT

We report here on results of AFM microscopy using laserless MEMS based probes. This new concept of Atomic Force Microscope (AFM) probes using bulk-mode silicon resonators was previously presented [1]. They consist on silicon ring resonators with capacitive transducers and integrated sensing nanotip. We have also demonstrated that these probes are sensitive to nanoscale tip-surface interactions [2], paving the way for AFM imaging. We describe here probes fabrication and their implementation on a Veeco commercial AFM microscope. Force curve measurements are realized in order to set the experimental conditions for AFM operation. For the first time, AFM microscopy images using these laserless MEMS based AFM probes are presented.

INTRODUCTION

Commercial AFM cantilevers make measurements with piconewton force sensitivity in vacuum but suffer from a drastic decrease of performances in liquids. Both the resonance frequency and the quality factor of the cantilevers are strongly degraded by viscosity forces. Probes using bulk-mode silicon resonators have higher resonance frequencies and higher quality factors [3], [4], [5], [6] compared to conventional AFM probes based on cantilevers [7]. So high rate imaging and more sensitive measurements in a liquid environment should be achieved with MEMS-based probes, thanks to the reduction of the effects of the viscosity forces [8]. In particular, resonator interactions with an external hydrodynamical force have been evaluated by measuring the resonator frequency response when the probe tip was dipped into a water droplet [9]. Tip-matter interactions measurements have also been evidenced by acquiring the output signal of the MEMS resonator when the tip was approached to and retracted from a surface [2]. These preliminary works confirmed that AFM microscopy could be achieved with MEMS probes. In this work, we describe the next step consisting in the implementation of these new MEMS based probes on a commercial AFM microscope. AFM images will be presented as a first proof of concept.

In a first part, we present the probe design and fabrication. Then in a second part, we describe their implementation in an AFM set-up. And finally we report AFM images made with MEMS-based AFM probes.

PROBE DESIGN AND FABRICATION

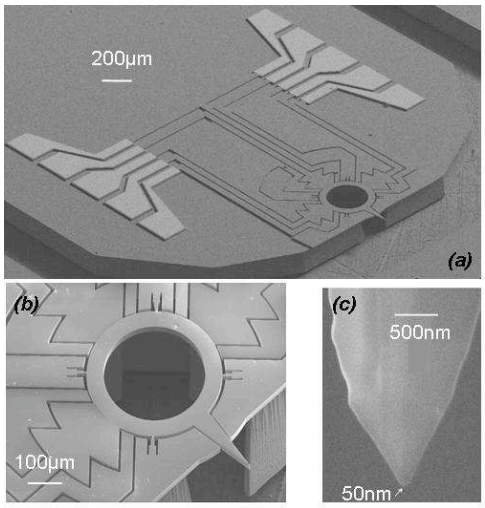

Figure 1: SEM images of a 250μm radius resonator based probe with tip length of 200μm. (a) overview of the device, (b) zoom on the ring resonator, (c) close view of the tip after FIB etching.

We fabricated devices with resonance frequencies at about 1 MHz in order to accommodate at first the bandwidth limitation of the commercial AFM set-up in which the probes were integrated. The probe (Fig.1) is made of a silicon ring resonator with capacitive transducers and an integrated nanotip. According to ANSYS simulation, 200 μm and 250 μm-radius rings were designed to obtain resonance frequencies at the vicinity of 1 MHz for the desired elliptic mode shape (Fig.2). We have developed a robust

fabrication process with few mask levels. MEMS-based AFM probes were fabricated from SOI wafers using photolithography and deep reactive ion etching (Fig. 3). The tip shape was post-processed by focused ion beam (FIB) to be sensitive to nanoscale interaction with a surface. After FIB etching, the radius of the tip apex is about 50nm (Fig.1c).

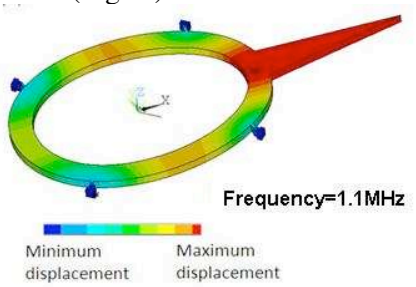

Figure 2: ANSYS modal simulation results: displacement of a 250 μm radius ring for the elliptic mode at 1.1 MHz.

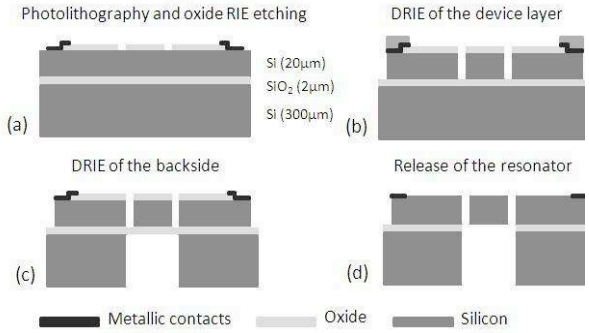

Figure 3: Process fabrication of the MEMS-based AFM probe. (a) The resonator structure is defined in the thermal oxide layer by photolithography and RIE etching, the metallic contacts are formed by lift-off. (b) The resonator structure is transferred in the silicon device layer by deep reactive ion etching. (c) The silicon handle layer is opened under the resonator by deep reactive ion etching. (d) The buried oxide layer is etched in a BOE solution and the resonator is released.

PROBE INTEGRATION IN AN AFM SET-UP

These probes were implemented on a commercially available AFM set-up (Fig.4). Our experimental set-up is made of a piezoelectric scanner from a Multimode Veeco AFM microscope and of a Nanonis controller controller to acquire the signals and to operate the feedback loop control. The microscope is placed on antivibration table. The probe holder of the Multimode Veeco microscope [10] is replaced by a dedicated circuit board supporting the MEMS probe. The Nanonis controller [11] drives the ring resonator and processes its output signal thanks to a lock-in amplifier. It also controls the XYZ Veeco scanner to realize 3D topography of the surface.

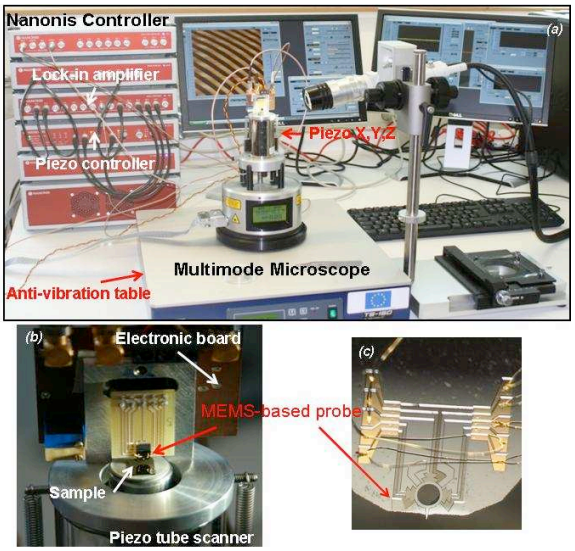

Figure 4: (a) Overview of the experimental set-up consisting of a Multimode Veeco microscope scanner, a Nanonis Controller and MEMS based probes mounted on a dedicated printed circuit board replacing the Veeco probe holder. (b) close view of the MEMS-based probe holder. (c) close view of the probe chip and bondings.

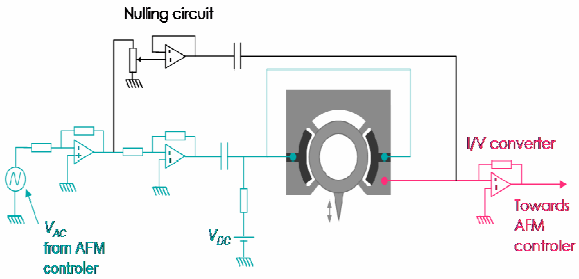

Figure 5: Schematic of the electronic circuit board.

The electronic board, on which the MEMS probe is placed, enables to drive ring resonator vibration and to process its output signal. (Fig.4(b) and Fig.5). The vibration plane of the ring resonator is oriented along the normal of the surface to probe. The elliptic vibration of the ring is driven thanks to an AC voltage and a DC bias voltage. The tip has then a vertical displacement with respect to the sample surface. As detailed later, when the tip is in intermittent contact with the surface, the ring resonance frequency and vibration amplitude change. The MEMS output current, which is proportional to the ring displacement velocity, is sensed through a

contact wired along to the anchors (Fig.4(c)). The electronic circuit board (Fig.5) convert the resonator output current into a voltage and allows to suppress the parasitic crosstalk (Fig.5). The lock-in amplifier enables to demodulate this voltage at the driving frequency and gives the signal amplitude and phase.

The mechanical resonance of the probe was characterized by using the microscope controller. The figure 6 shows the frequency response of a probe operating at 1.101 MHz. The AC driving voltage and the DC bias are respectively equal to 0.5 V and 12V. Depending on the device design, resonance frequencies have been measured between 0.9 and 1.6 MHz with quality factor ranging from 500 to 2200.

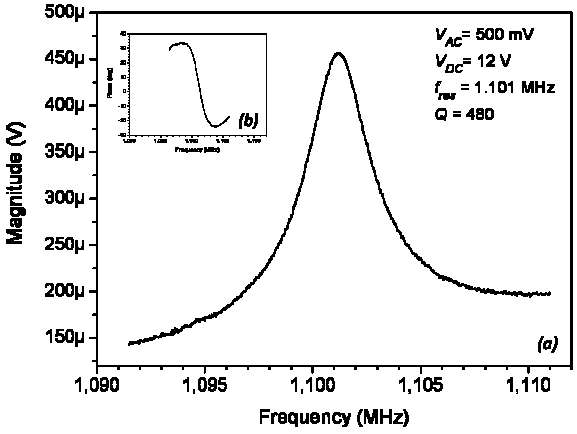

Figure 6: Electrical characteristic measured on a fabricated resonator with a bias voltage of 12 V, a driving voltage of 500mV (a) output signal amplitude (b) output signal phase. The resonance frequency is 1.101MHz

Subsequently, force curve measurements were performed to evaluate the sensitivity of the probe regarding surface interactions (Fig.7). The output signal amplitude is measured when the probe is approached to a silicon surface thanks to the Z piezoelectric scanner while the resonator is driven close to its resonance frequency. Far away the surface the output signal amplitude is constant and equal to the free amplitude signal. Then, while the tip is in intermittent contact with the surface, it sense the nanoscale interactions and the output signal amplitude decreases when the tip-sample is reduced. Finally when the resonator permanently contacts the surface, oscillation vanishes. The tip oscillation amplitude can be estimated to a few nanometers, by measuring the extension of the intermittent contact regime.

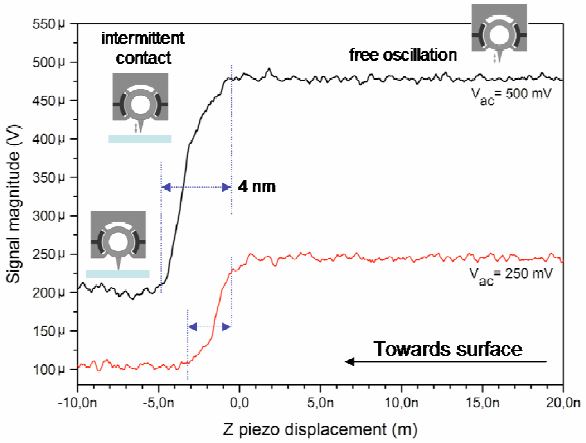

Figure 7: Measurement of the vibration amplitude when the tip is approached to a silicon surface for two driving voltages.

AFM MICROSCOPY USING MEMS PROBES

Finally, we realized first AFM images with the probes. The tip-surface distance is adjusted by the Nanonis feedback control loop to keep the resonator signal amplitude equal to a given setpoint lower than the free oscillation amplitude. According to curve force measurements (Fig. 7), parameters for imaging were chosen. In particular the setpoint amplitude was chosen to be equal to 80% of the free amplitude in order to keep a weak surface interaction with the surface.

By scanning the X and Y axis and acquiring the Z regulation signal, topographic images of the surface sample were obtained. To validate our approach, some test samples were fabricated. The first one is formed of trenches etched in silicon with a depth of 250nm. The Figure 8 presents AFM images of these 2 μm width silicon trenches separated by 1 μm. They were realized with a probe operating at 936 kHz and a scan speed of 1 μm/s and 2 μm/s for the 5 μm and 10 μm width image respectively. To evaluate capability of our probe to image nanoscale patterns, a sample were fabricated by e-beam lithography. The Figure 9 shows 3D topography of 100 nm wide, 30 nm high silicon lines separated by 400 nm. These images were realized with 942 kHz probe and scan speed of 100 nm/s and 200 nm/s.

These results demonstrate that patterns featuring sub-100 nm lateral dimensions can be successfully imaged using the MEMS-based AFM probes.

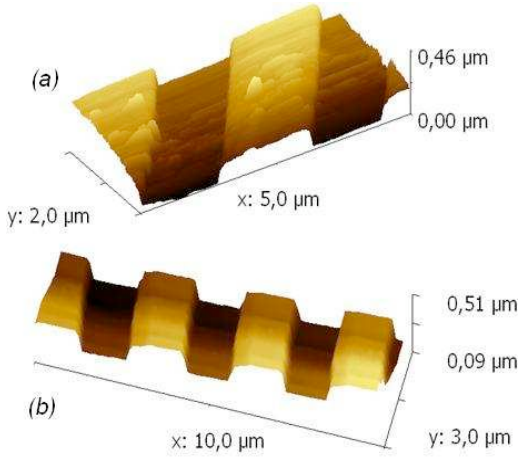

Figure 8: AFM images of 1 μm wide, 250 nm high silicon patterns (spacing = 1 μm) acquired with a 936 kHz MEMS-based probe (V_{DC}=15 V, V_{AC}=500 mV). Tip scan rate is 1 μm/s (a) and 2 μm/s (b).

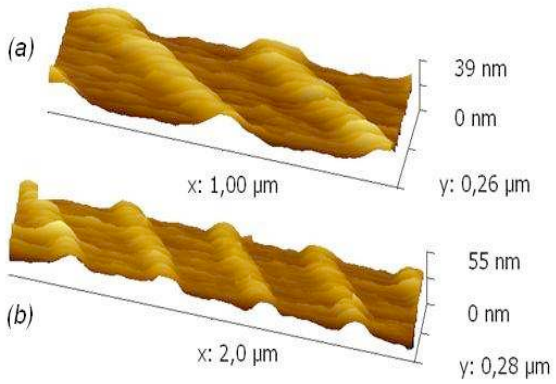

Figure 9: AFM images of 100 nm wide, 30 nm high silicon patterns (spacing = 400 nm) acquired with a 936 kHz MEMS-based probe (V_{DC}=25 V, V_{AC}=500 mV). Tip scan rate is 100 nm/s (a) and 200 nm/s (b).

CONCLUSION AND PROSPECTS

We have modified a commercial AFM set-up to implement the fabricated laserless MEMS based probes. We have demonstrated AFM microscopy with these new performing MEMS probes. Images have been obtained on 100 nm-wide patterns with probes featuring 50 nm tip apex. Current work aims at improving the lateral resolution by using sharper tips. We are also focusing on downscaling the devices to reach higher frequencies up to the GHz range. This should enable to achieve higher acquisition rate and to perform AFM microscopy and spectroscopy in liquid.

Acknowledgement
This work is funded by the ANR project "Improve-LM" and the research leading to the results has received funding from the European community's Seventh Framework Program (FP7/2007-2013 Grant Agreement no.210078).

Corresponding author
Bernard Legrand, NAM6 group, IEMN - CNRS UMR8520, Villeneuve d'Ascq, FRANCE
Tel: +33 320 197 948 Email:
bernard.legrand@isen.iemn.univ-lille1.fr

REFERENCES

[1] M. Faucher, B. Walter, A.-S. Rollier, K. Segueni, B. Legrand, G. Couturier, J.-P. Aime, C. Bernard, R. Boisgard and L. Buchaillot, Proc. of the Transducers'07 Conference, Lyon, France, June 10-14, 2007, pp. 1529-1532

[2] E. Algré, B. Legrand, M. Faucher, B. Walter, L. Buchaillot, Proc. Of the Transducers'09 Conference, Denver, USA, June 21-25, 2009, pp. 1638 -1641

[3] J. Wang, C. T.-C. Nguyen, IEEE Trans. Ultrasonics, vol. 51 (12), pp.1607, 2004

[4] Z. Hao, S. Pourkamali, F. Ayazi, J. Microelectromech. Syst, vol. 13, pp. 1043, 2004

[5] S. Pourkamali, Z. Hao F. Ayazi, J. Microelectromech. Syst., vol. 13, pp. 1054, 2004

[6] M. U. Demerci, C. T.-C. Nguyen, J. Microelectromech. Syst., vol. 15, pp. 1419, 2006

[7] T. R. Albrecht, S. Akamine, T. E. Carver, C. Quate, J. Vac. Sci. A, vol. 8, pp. 3386, 1990

[8] A. Maali, C. Hurth, R. Boisgard, C. Jai, T. Cohen-Bouhacina, and J.-P. Aimé, J. Appl. Phys. , vol. 97, pp. 074907, 2005

[9] B. Walter, M. Faucher, E. Algré, B. Legrand, R. Boisgard, J.-P. Aimé and L. Buchaillot, J. Micromech. Microeng., vol. 19, pp. 115009, 2009

[10] www.veeco.com

[11] www.nanonis.com